Supplementary Material (ESI) for PCCP

Supporting Information for
Non-Classical Diffusion in Ionic Liquids

Alasdair W. Taylor,[a] Peter Licence[*a] and Andrew P. Abbott[*b]

[a]School of Chemistry, The University of Nottingham, Nottingham NG7 2RD, UK

[b]Department of Chemistry, University of Leicester, Leicester LE1 7RH, UK

*To whom correspondence should be addressed:

peter.licence@nottingham.ac.uk

Tel: +44 115 8466176

[FcC$_1$C$_1$Im][Tf$_2$N] in [C$_4$C$_1$Im][Tf$_2$N]

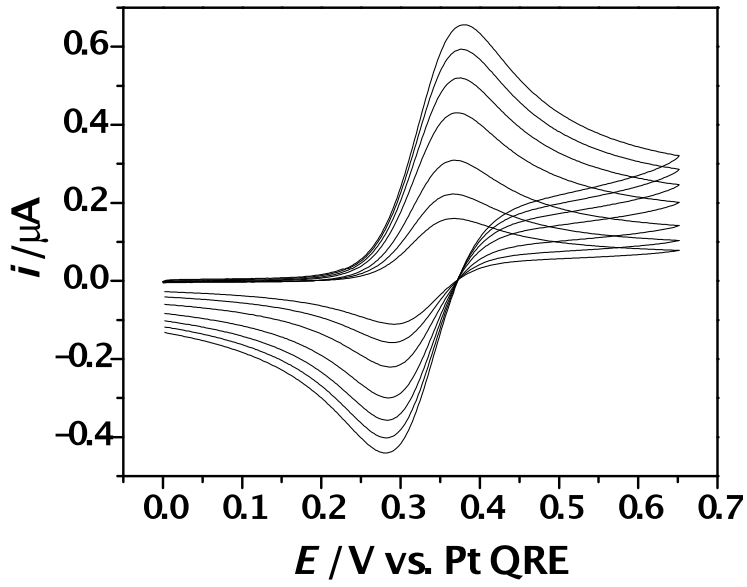

Figure S1 *CVs obtained at WE1 in a 4.59 mM solution of [FcC$_1$C$_1$Im][Tf$_2$N] in [C$_4$C$_1$Im][Tf$_2$N], ν ranged from 25-500 mV s^{-1}, T = 298 K, p = 5 × 10^{-6} mbar.*

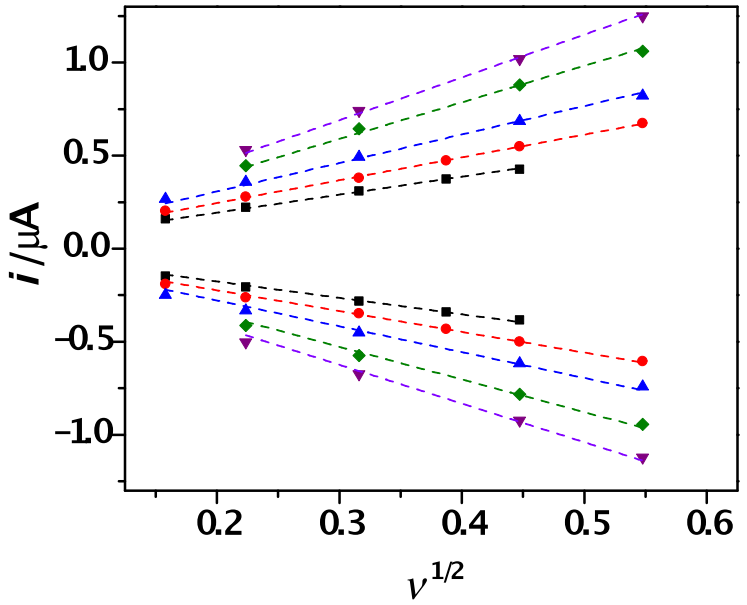

Figure S2 *Randles-Sevçik plots of $i_{p,a}$ and $i_{p,c}$ vs. $\nu^{1/2}$ at T = 298 K (—), 313 K (—), 330 K (—), 348 K (—) and 363 K (—).*

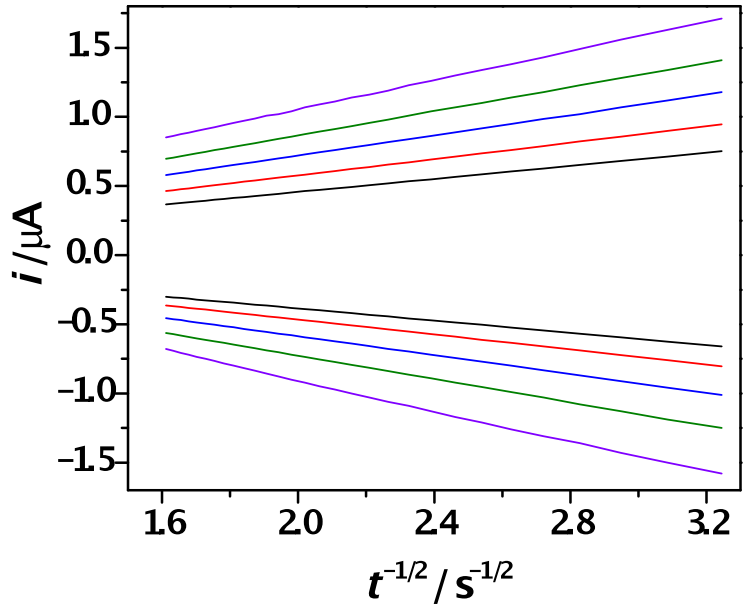

Figure S3 *Cottrell plots generated from the chronoamperometric curves obtained at WE2 in a 4.74 mM solution of [FcC$_1$C$_1$Im][Tf$_2$N] in [C$_4$C$_1$Im][Tf$_2$N], T = 298 K (—), 313 K (—), 330 K (—), 348 K (—) and 363 K (—), p = 5 × 10^{-6} mbar.*

Table S1 *Diffusion coefficients obtained for the oxidised and reduced forms of [FcC$_1$C$_1$Im][Tf$_2$N] in [C$_4$C$_1$Im][Tf$_2$N] using CV and chronoamperometry recorded at different temperatures.*

T / K	D_{RS} $[FcC_1C_1Im]^+$ $\times 10^{-7}$ cm^2 s^{-1}	D_{RS} $[Fc^+C_1C_1Im]^{2+}$ $\times 10^{-7}$ cm^2 s^{-1}	D_{Cott} $[FcC_1C_1Im]^+$ $\times 10^{-7}$ cm^2 s^{-1}	D_{Cott} $[Fc^+C_1C_1Im]^{2+}$ $\times 10^{-7}$ cm^2 s^{-1}
298	0.74 ± 0.03	0.62 ± 0.02	1.09 ± 0.06	1.00 ± 0.05
313	1.25 ± 0.04	1.12 ± 0.04	1.73 ± 0.08	1.50 ± 0.07
330	2.06 ± 0.08	1.69 ± 0.07	2.68 ± 0.12	2.40 ± 0.11
348	3.58 ± 0.14	2.85 ± 0.11	3.87 ± 0.18	3.66 ± 0.17
363	5.10 ± 0.19	4.19 ± 0.17	5.73 ± 0.26	6.36 ± 0.29

[FcC_1C_1Im][Tf_2N] in [C_8C_1Im][Tf_2N]

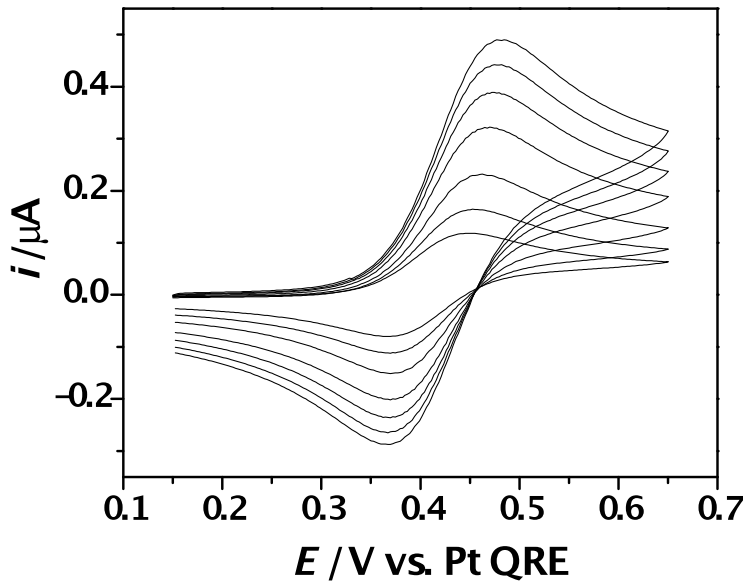

Figure S4 *CVs obtained at WE1 in a 4.88 mM solution of [FcC_1C_1Im][Tf_2N] in [C_8C_1Im][Tf_2N], v ranged from 25-500 mV s^{-1}, T = 298 K, p = 5 × 10^{-6} mbar.*

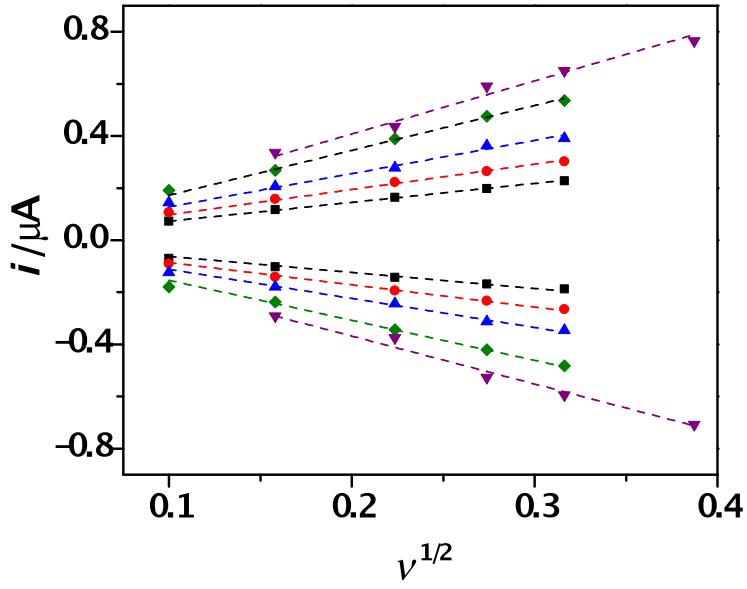

Figure S5 *Randles-Sevçik plots of $i_{p,a}$ and $i_{p,c}$ vs. $v^{1/2}$ at T = 298 K (—), 313 K (—), 330 K (—), 348 K (—) and 363 K (—).*

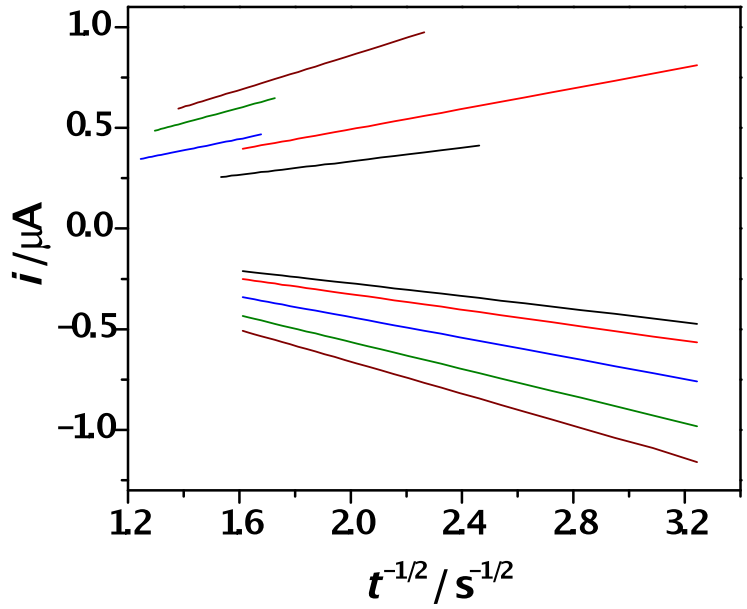

Figure S6 *Cottrell plots generated from the chronoamperometric curves obtained at WE2 in a 4.34 mM solution of [FcC$_1$C$_1$Im][Tf$_2$N] in [C$_8$C$_1$Im][Tf$_2$N], T = 298 K (—), 313 K (—), 330 K (—), 348 K (—) and 363 K (—), p = 5 × 10^{-6} mbar.*

Table S2 *Diffusion coefficients obtained for the oxidised and reduced forms of [FcC$_1$C$_1$Im][Tf$_2$N] in [C$_8$C$_1$Im][Tf$_2$N] using CV and chronoamperometry recorded at different temperatures.*

T / K	D_{RS} $[FcC_1C_1Im]^+$ $\times 10^{-7}$ cm^2 s^{-1}	D_{RS} $[Fc^+C_1C_1Im]^{2+}$ $\times 10^{-7}$ cm^2 s^{-1}	D_{Cott} $[FcC_1C_1Im]^+$ $\times 10^{-7}$ cm^2 s^{-1}	D_{Cott} $[Fc^+C_1C_1Im]^{2+}$ $\times 10^{-7}$ cm^2 s^{-1}
298	0.37 ± 0.01	0.27 ± 0.01	0.68 ± 0.03	0.63 ± 0.03
313	0.70 ± 0.03	0.54 ± 0.02	1.50 ± 0.07	0.92 ± 0.05
330	1.27 ± 0.05	0.97 ± 0.04	1.89 ± 0.09	1.61 ± 0.08
348	2.43 ± 0.09	1.93 ± 0.08	3.44 ± 0.16	2.76 ± 0.13
363	3.55 ± 0.15	2.89 ± 0.12	4.55 ± 0.22	3.89 ± 0.18

A2.1 [FcC₁C₁Im][Tf₂N] in [C₂C₁Im][BF₄]

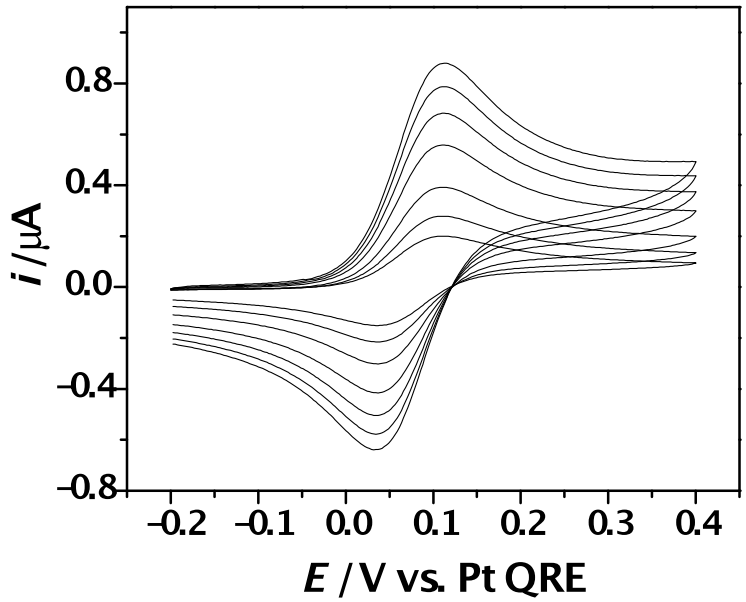

Figure S7 *CVs obtained at WE1 in a 4.56 mM solution of [FcC1C1Im][Tf2N] in [C2C1Im][BF4], ν ranged from 25-500 mV s-1, T = 298 K, p = 5 × 10-6 mbar.*

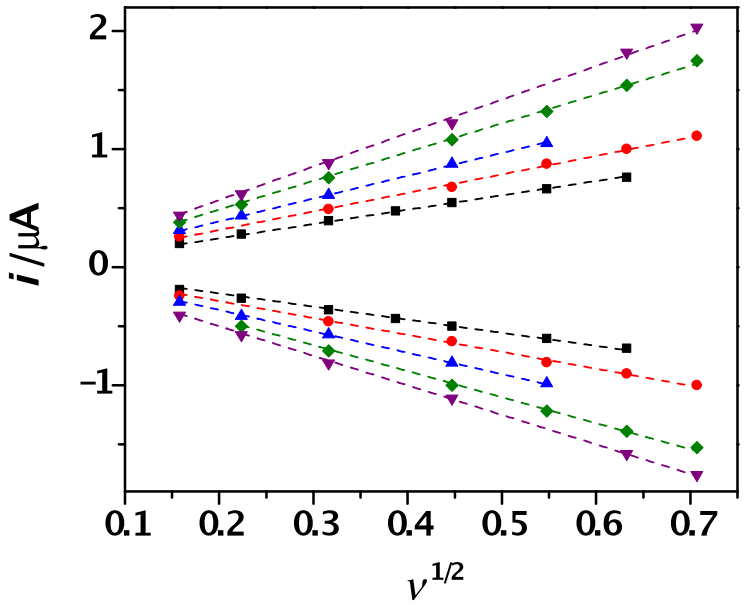

Figure S8 *Randles-Sevçik plots of $i_{p,a}$ and $i_{p,c}$ vs. $\nu^{1/2}$ at T = 298 K (—), 313 K (—), 330 K (—), 348 K (—) and 363 K (—).*

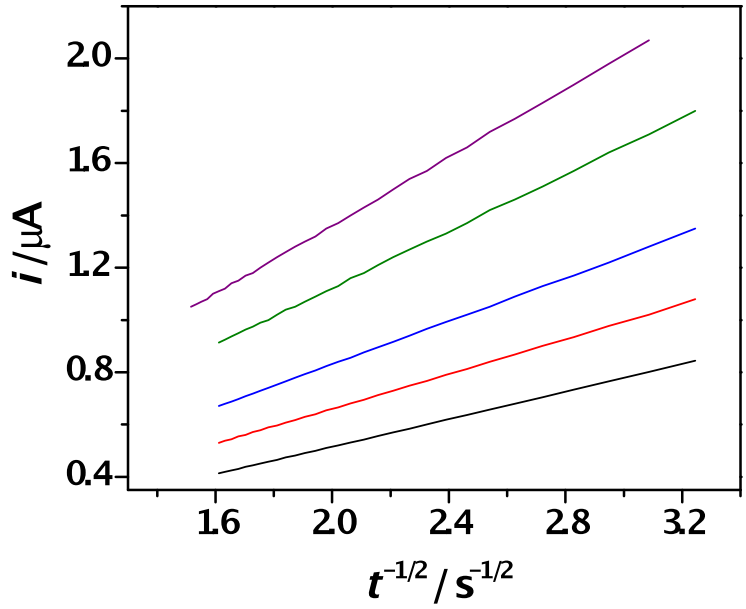

Figure S9 *Cottrell plots generated from the chronoamperometric curves obtained at WE2 in a 4.36 mM solution of [FcC$_1$C$_1$Im][Tf$_2$N] in [C$_2$C$_1$Im][BF$_4$], T = 298 K (—), 313 K (—), 330 K (—), 348 K (—) and 363 K (—), p = 5 × 10^{-6} mbar.*

Table S3 *Diffusion coefficients obtained for the oxidised and reduced forms of [FcC$_1$C$_1$Im][Tf$_2$N] in [C$_2$C$_1$Im][BF$_4$] using CV and chronoamperometry recorded at different temperatures.*

T / K	D_{RS} $[FcC_1C_1Im]^+$ $\times 10^{-7}$ cm^2 s^{-1}	D_{RS} $[Fc^+C_1C_1Im]^{2+}$ $\times 10^{-7}$ cm^2 s^{-1}	D_{Cott} $[FcC_1C_1Im]^+$ $\times 10^{-7}$ cm^2 s^{-1}
298	1.19 ± 0.04	0.99 ± 0.04	1.62 ± 0.07
313	2.08 ± 0.07	1.74 ± 0.06	2.66 ± 0.12
330	3.26 ± 0.12	2.92 ± 0.11	4.18 ± 0.19
348	5.55 ± 0.20	4.55 ± 0.17	8.62 ± 0.40
363	7.87 ± 0.30	6.11 ± 0.23	11.24 ± 0.50

[FcC_1C_1Im][Tf_2N] in [C_4C_1Im][BF_4]

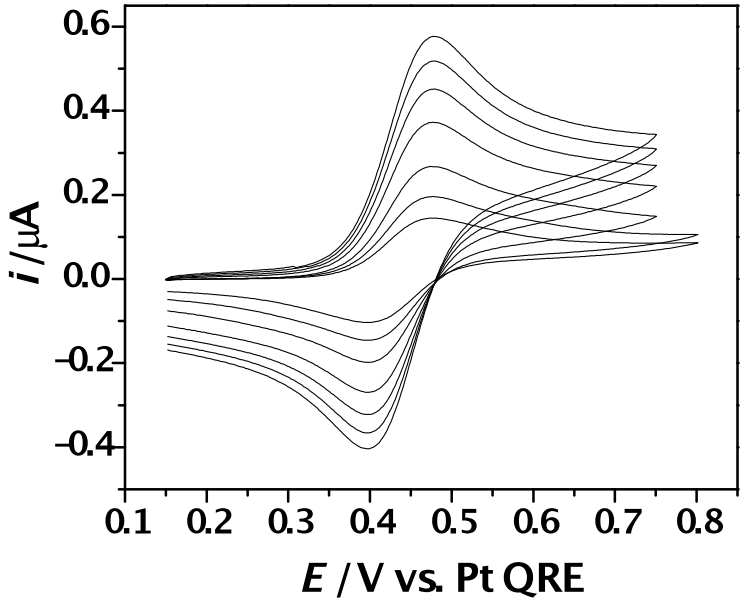

Figure S10 *CVs obtained at WE1 in a 4.66 mM solution of [FcC_1C_1Im][Tf_2N] in [C_4C_1Im][BF_4], ν ranged from 25-500 mV s^{-1}, T = 298 K, p = 5 × 10^{-6} mbar.*

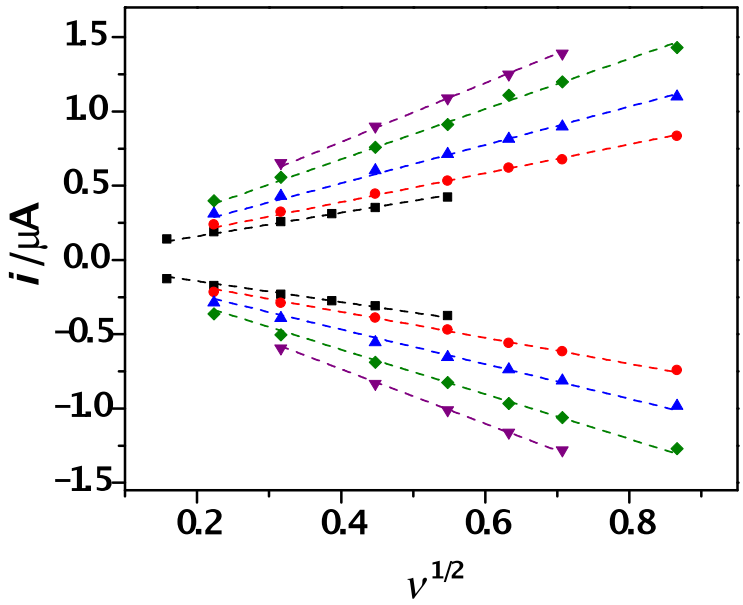

Figure S11 *Randles-Sevçik plots of $i_{p,a}$ and $i_{p.c}$ vs. $\nu^{1/2}$ at T = 298 K (—), 313 K (—), 330 K (—), 348 K (—) and 363 K (—).*

Table S4 *Diffusion coefficients obtained for the oxidised and reduced forms of [FcC_1C_1Im][Tf_2N] in [C_4C_1Im][BF_4] using CV recorded at different temperatures.*

T / K	D_{RS} $[FcC_1C_1Im]^+$ $\times 10^{-7}$ cm^2 s^{-1}	D_{RS} $[Fc^+C_1C_1Im]^{2+}$ $\times 10^{-7}$ cm^2 s^{-1}
298	0.49 ± 0.02	0.38 ± 0.01
313	0.76 ± 0.03	0.62 ± 0.02
330	1.42 ± 0.05	1.16 ± 0.04
348	2.63 ± 0.10	2.08 ± 0.08
363	3.7 ± 0.14	3.15 ± 0.12

[FcC_1C_1Im][Tf_2N] in [C_8C_1Im][BF_4]

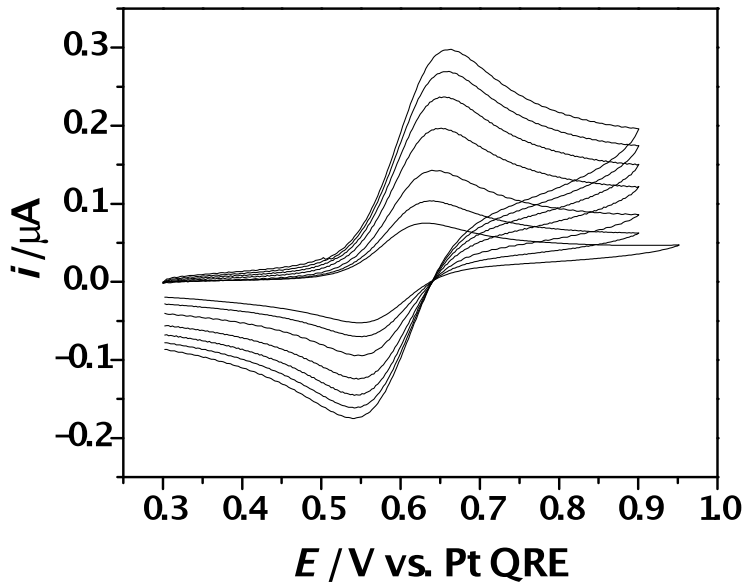

Figure S12 *CVs obtained at WE1 in a 4.66 mM solution of [FcC_1C_1Im][Tf_2N] in [C_8C_1Im][BF_4], ν ranged from 25-500 mV s^{-1}, T = 298 K, p = 5 × 10^{-6} mbar.*

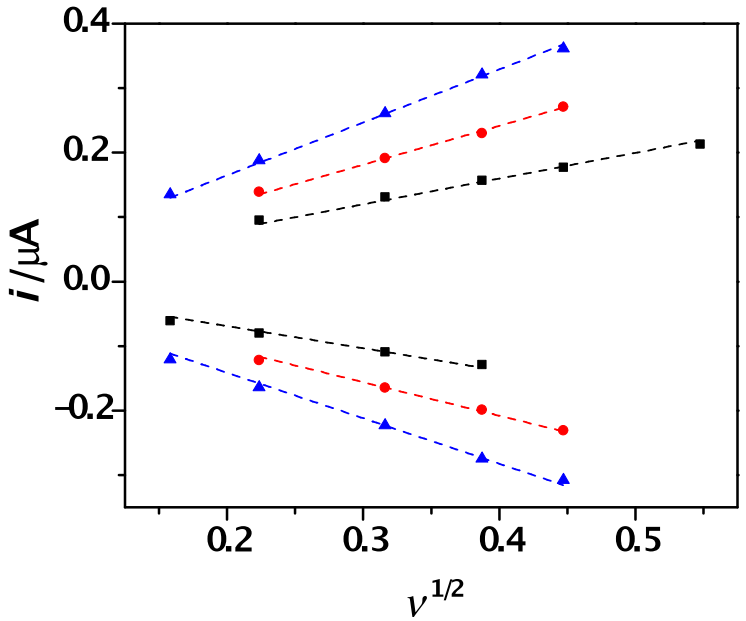

Figure S13 *Randles-Sevçik plots of $i_{p,a}$ and $i_{p,c}$ vs. $\nu^{1/2}$ at T = 298 K (—), 313 K (—), and 330 K (—).*

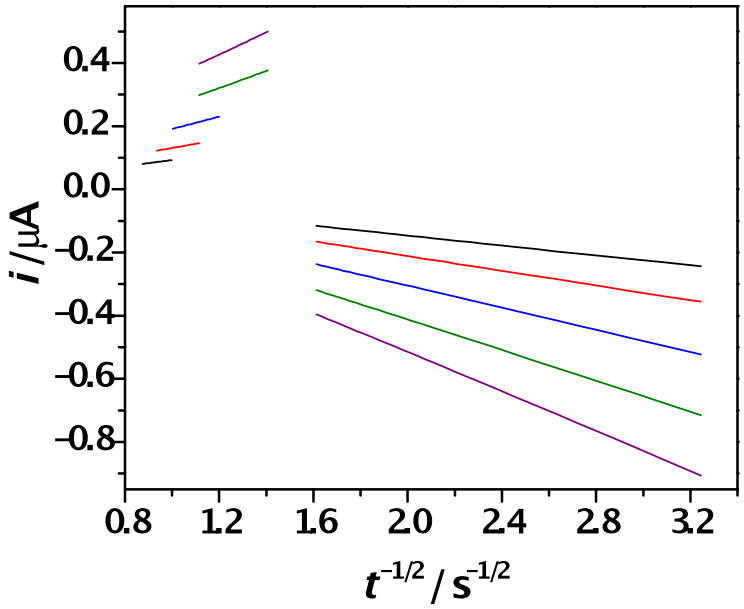

Figure S14 *Cottrell plots generated from the chronoamperometric curves obtained at WE2 in a 4.36 mM solution of [FcC$_1$C$_1$Im][Tf$_2$N] in [C$_8$C$_1$Im][BF$_4$], T = 298 K (—), 313 K (—), 328 K (—), 348 K (—) and 363 K (—), p = 5 × 10^{-6} mbar.*

Table S5 *Diffusion coefficients obtained for the oxidised and reduced forms of [FcC$_1$C$_1$Im][Tf$_2$N] in [C$_8$C$_1$Im][BF$_4$] using CV and chronoamperometry recorded at different temperatures.*

T / K	D_{RS} $[FcC_1C_1Im]^+$ $\times 10^{-8}$ cm^2 s^{-1}	D_{RS} $[Fc^+C_1C_1Im]^{2+}$ $\times 10^{-8}$ cm^2 s^{-1}	D_{Cott} $[FcC_1C_1Im]^+$ $\times 10^{-8}$ cm^2 s^{-1}	D_{Cott} $[Fc^+C_1C_1Im]^{2+}$ $\times 10^{-8}$ cm^2 s^{-1}
298	1.2 ± 0.1	0.9 ± 0.1	1.9 ± 0.1	1.4 ± 0.1
313	2.8 ± 0.1	2.1 ± 0.1	3.8 ± 0.2	3.0 ± 0.1
330	5.4 ± 0.2	4.0 ± 0.2	8.1 ± 0.4	6.7 ± 0.3
348	-	-	15.7 ± 0.7	12.9 ± 0.6
363	-	-	27.8 ± 1.3	21.4 ± 1.0

$[FcC_1C_1Im][Tf_2N]$ in $[C_4C_1Im][PF_6]$

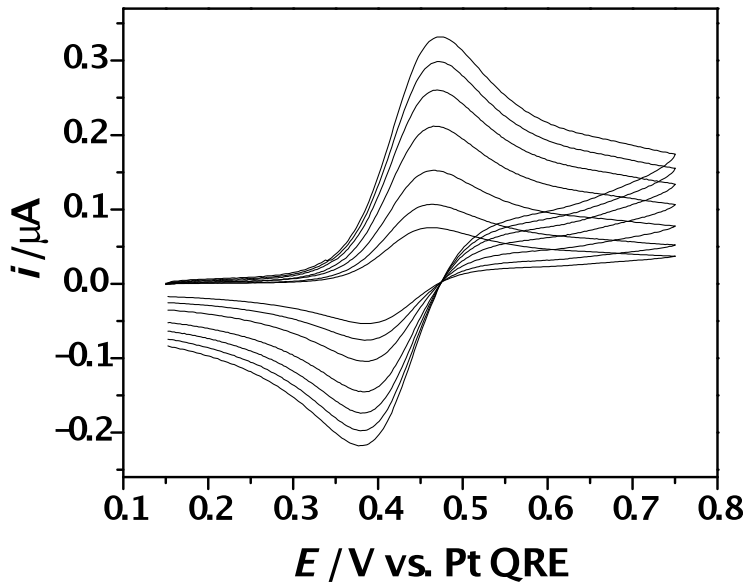

Figure S15 *CVs obtained at WE1 in a 4.20 mM solution of $[FcC_1C_1Im][Tf_2N]$ in $[C_4C_1Im][PF_6]$, ν ranged from 25-500 mV s^{-1}, T = 298 K, p = 5 × 10^{-6} mbar.*

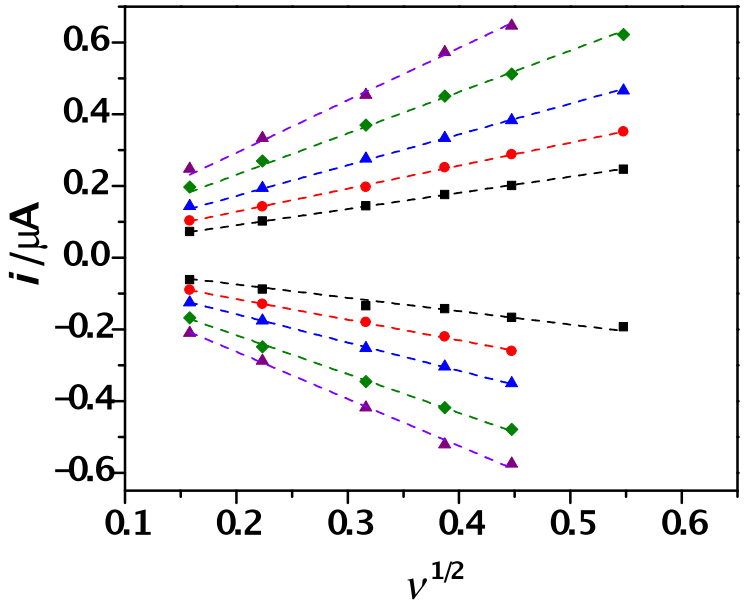

Figure S16 *Randles-Sevçik plots of $i_{p,a}$ and $i_{p,c}$ vs. $\nu^{1/2}$ at T = 298 K (—), 313 K (—), 330 K (—), 348 K (—) and 363 K (—).*

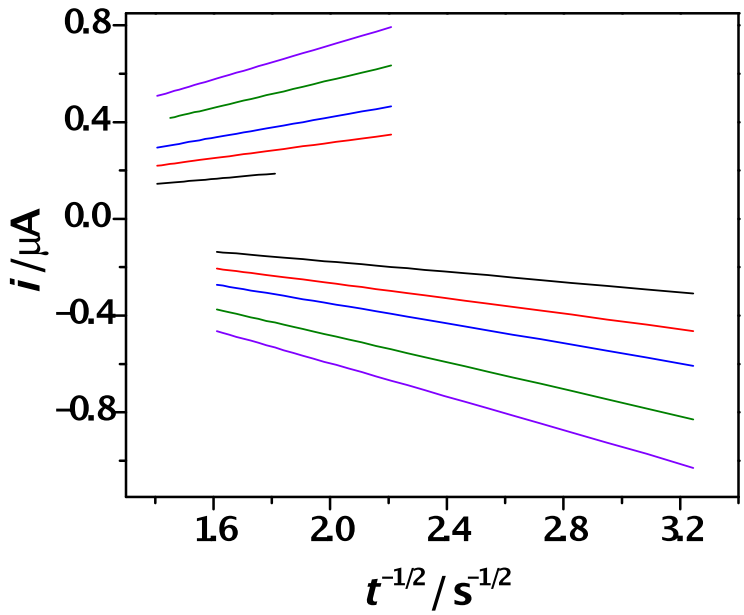

Figure S17 *Cottrell plots generated from the chronoamperometric curves obtained at WE2 in a 4.38 mM solution of [FcC$_1$C$_1$Im][Tf$_2$N] in [C$_4$C$_1$Im][PF$_6$], T = 298 K (—), 318 K (—), 330 K (—), 348 K (—) and 363 K (—), p = 5 × 10^{-6} mbar.*

Table S6 *Diffusion coefficients obtained for the oxidised and reduced forms of [FcC$_1$C$_1$Im][Tf$_2$N] in [C$_4$C$_1$Im][PF$_6$] using CV and chronoamperometry recorded at different temperatures.*

T / K	D_{RS} $[FcC_1C_1Im]^+$ $\times 10^{-8}$ cm^2 s^{-1}	D_{RS} $[Fc^+C_1C_1Im]^{2+}$ $\times 10^{-8}$ cm^2 s^{-1}	D_{Cott} $[FcC_1C_1Im]^+$ $\times 10^{-8}$ cm^2 s^{-1}	D_{Cott} $[Fc^+C_1C_1Im]^{2+}$ $\times 10^{-8}$ cm^2 s^{-1}
298	1.9 ± 0.1	1.3 ± 0.1	2.6 ± 0.1	2.7 ± 0.2
313	4.1 ± 0.1	3.3 ± 0.1	-	-
318	-	-	6.0 ± 0.3	6.0 ± 0.3
330	7.7 ± 0.3	6.5 ± 0.2	10.6 ± 0.5	10.1 ± 0.5
348	14.5 ± 0.5	13.0 ± 0.5	19.9 ± 1.0	18.7 ± 0.8
363	24.6 ± 0.9	19.9 ± 0.8	31.2 ± 1.4	28.6 ± 1.3

$[FcC_1C_1Im][Tf_2N]$ in $[C_8C_1Im][PF_6]$

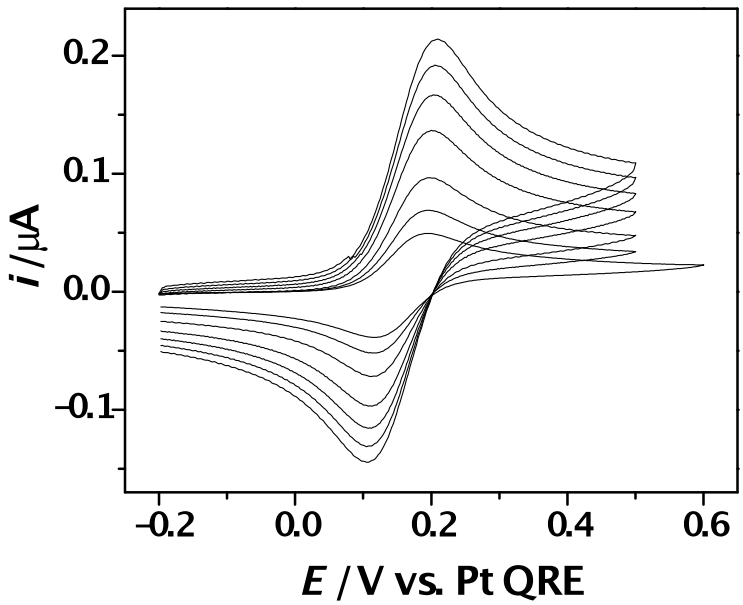

Figure S18 *CVs obtained at WE1 in a 4.74 mM solution of $[FcC_1C_1Im][Tf_2N]$ in $[C_8C_1Im][PF_6]$, ν ranged from 25-500 mV s^{-1}, T = 298 K, p = 5 × 10^{-6} mbar.*

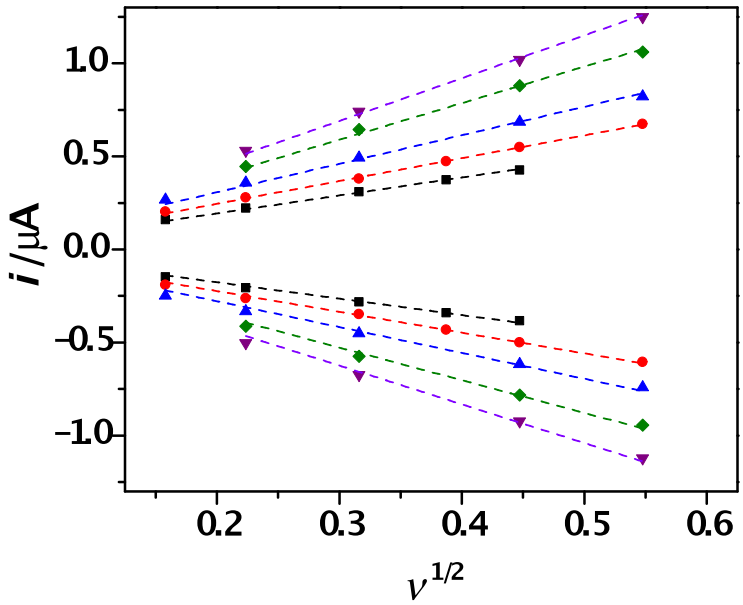

Figure S19 *Randles-Sevçik plots of $i_{p,a}$ and $i_{p,c}$ vs. $\nu^{1/2}$ at T = 298 K (—), 313 K (—), 330 K (—) and 348 K (—).*

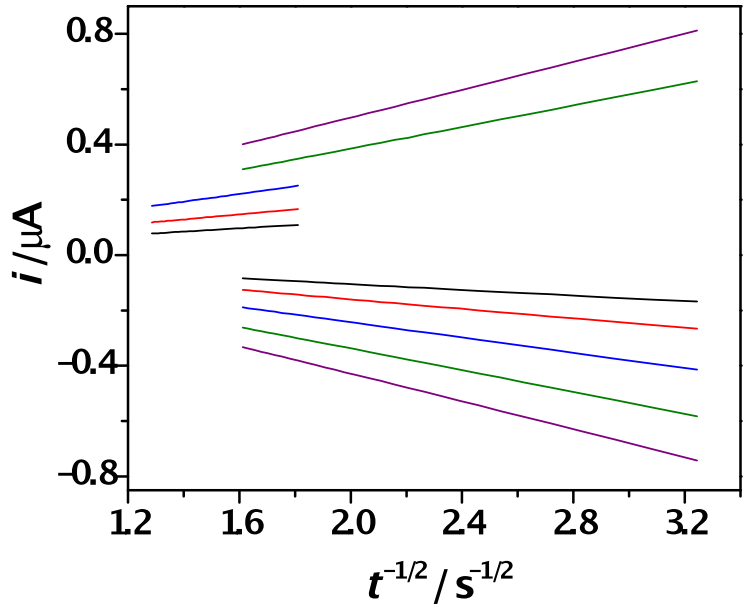

Figure S20 *Cottrell plots generated from the chronoamperometric curves obtained at WE2 in a 4.42 mM solution of [FcC$_1$C$_1$Im][Tf$_2$N] in [C$_8$C$_1$Im][PF$_6$], T = 298 K (—), 313 K (—), 330 K (—), 348 K (—) and 363 K (—), p = 5 × 10^{-6} mbar.*

Table S7 *Diffusion coefficients obtained for the oxidised and reduced forms of [FcC$_1$C$_1$Im][Tf$_2$N] in [C$_8$C$_1$Im][PF$_6$] using CV and chronoamperometry recorded at different temperatures.*

T / K	D_{RS} $[FcC_1C_1Im]^+$ $\times 10^{-8}$ cm^2 s^{-1}	D_{RS} $[Fc^+C_1C_1Im]^{2+}$ $\times 10^{-8}$ cm^2 s^{-1}	D_{Cott} $[FcC_1C_1Im]^+$ $\times 10^{-8}$ cm^2 s^{-1}	D_{Cott} $[Fc^+C_1C_1Im]^{2+}$ $\times 10^{-8}$ cm^2 s^{-1}
298	0.6 ± 0.1	0.5 ± 0.1	0.9 ± 0.1	0.7 ± 0.1
313	1.4 ± 0.1	1.2 ± 0.1	2.0 ± 0.1	1.8 ± 0.1
330	3.3 ± 0.1	2.8 ± 0.1	4.5 ± 0.2	4.5 ± 0.2
348	7.6 ± 0.3	6.6 ± 0.3	8.8 ± 0.4	9.1 ± 0.4
363	-	-	14.7 ± 0.7	14.9 ± 0.7

[FcC$_1$C$_1$Im][Tf$_2$N] in [C$_2$C$_1$Im][EtOSO$_3$]

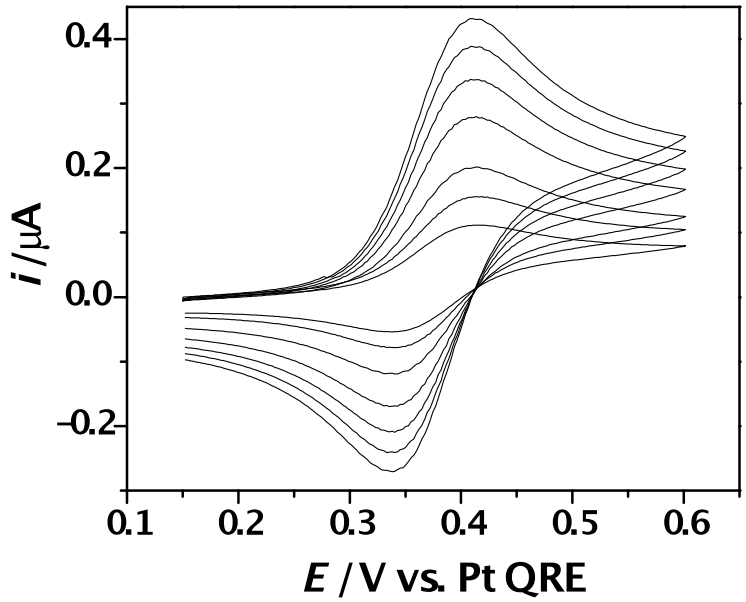

Figure S21 *CVs obtained at WE1 in a 4.44 mM solution of [FcC$_1$C$_1$Im][Tf$_2$N] in [C$_2$C$_1$Im][EtOSO$_3$], ν ranged from 25-500 mV s^{-1}, T = 298 K, p = 5 × 10^{-6} mbar.*

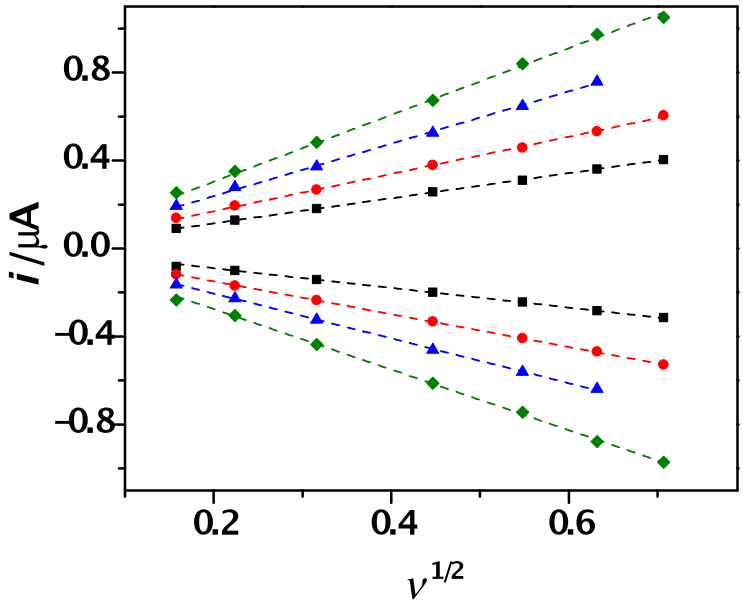

Figure S22 *Randles-Sevçik plots of $i_{p,a}$ and $i_{p,c}$ vs. $\nu^{1/2}$ at T = 298 K (—), 323 K (—), 348 K (—) and 373 K (—).*

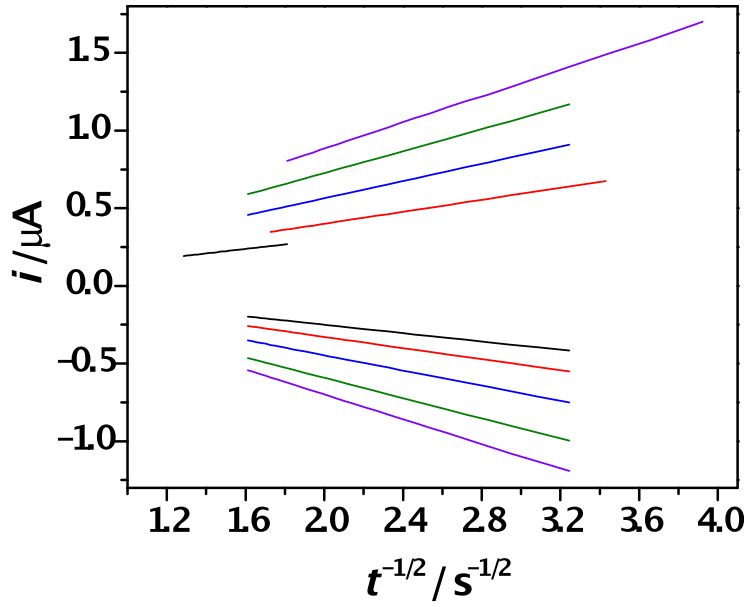

Figure S23 *Cottrell plots generated from the chronoamperometric curves obtained at WE2 in a 4.67 mM solution of $[FcC_1C_1Im][Tf_2N]$ in $[C_2C_1Im][EtOSO_3]$, T = 298 K (—), 313 K (—), 330 K (—), 348 K (—) and 363 K (—), p = 5 × 10^{-6} mbar.*

Table S8 *Diffusion coefficients obtained for the oxidised and reduced forms of $[FcC_1C_1Im][Tf_2N]$ in $[C_2C_1Im][EtOSO_3]$ using CV and chronoamperometry recorded at different temperatures.*

T / K	D_{RS} $[FcC_1C_1Im]^+$ $\times 10^{-7}$ cm^2 s^{-1}	D_{RS} $[Fc^+C_1C_1Im]^{2+}$ $\times 10^{-7}$ cm^2 s^{-1}	D_{Cott} $[FcC_1C_1Im]^+$ $\times 10^{-7}$ cm^2 s^{-1}	D_{Cott} $[Fc^+C_1C_1Im]^{2+}$ $\times 10^{-7}$ cm^2 s^{-1}
298	0.34 ± 0.01	0.24 ± 0.01	0.47 ± 0.02	0.39 ± 0.02
313	-	-	0.84 ± 0.04	0.68 ± 0.03
323	0.81 ± 0.03	0.63 ± 0.02	-	-
330	-	-	1.68 ± 0.07	1.27 ± 0.06
348	1.72 ± 0.06	1.26 ± 0.05	2.78 ± 0.13	2.27 ± 0.10
363	-	-	4.01 ± 0.19	3.37 ± 0.15
373	3.00 ± 0.12	2.46 ± 0.09	-	-

[FcC$_1$C$_1$Im][Tf$_2$N] in [C$_2$C$_1$Im][Tf$_2$N] with Ferrocene

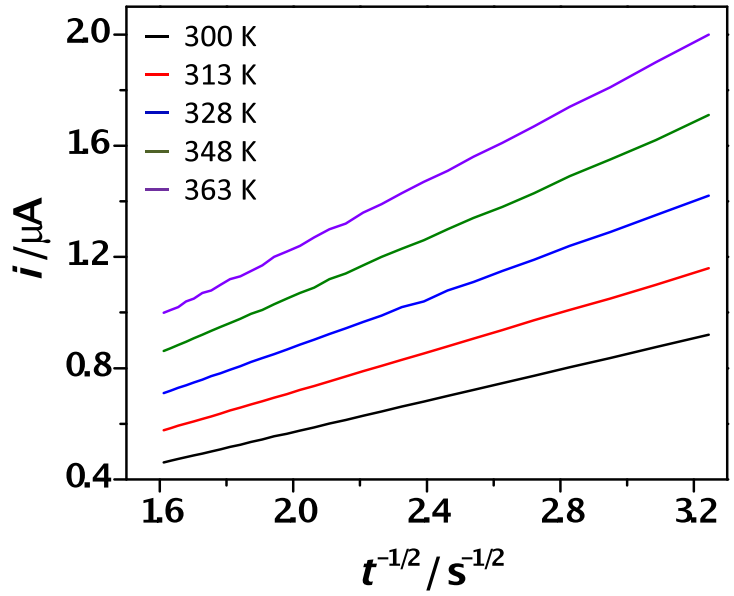

Figure S24 *Cottrell plots for the oxidation of [FcC$_1$C$_1$Im][Tf$_2$N] generated from the chronoamperometric curves obtained at WE2 in a 4.68 mM solution of [FcC$_1$C$_1$Im][Tf$_2$N] in [C$_2$C$_1$Im][Tf$_2$N], T = 300 K (—), 313 K (—), 328 K (—), 348 K (—) and 363 K (—), p = 5 × 10^{-6} mbar.*

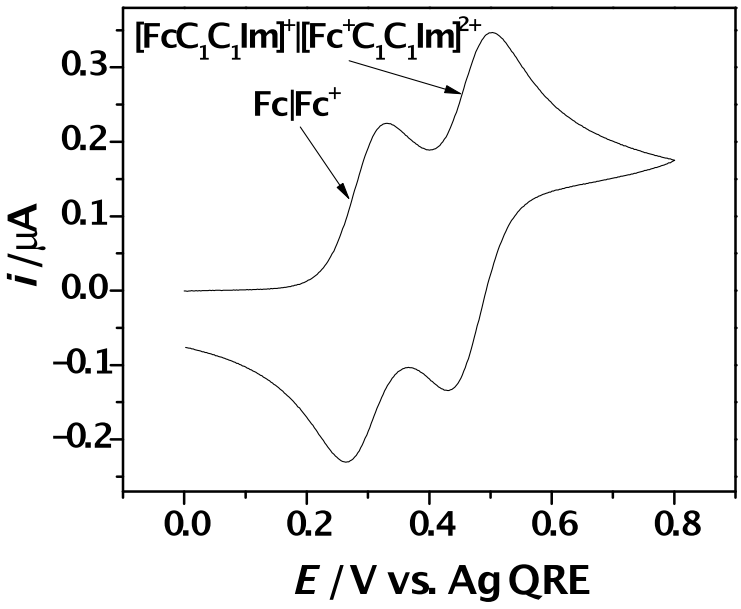

Figure S25 *CV recorded obtained at WE2 in a in a 4.48 mM solution of FcC$_1$Im in [C$_2$C$_1$Im][Tf$_2$N] doped with 2.54 mM ferrocene, ν = 50 mV s^{-1}, T = 298 K, p = 1 atm.*

FcC_1Im in $[C_2C_1Im][Tf_2N]$

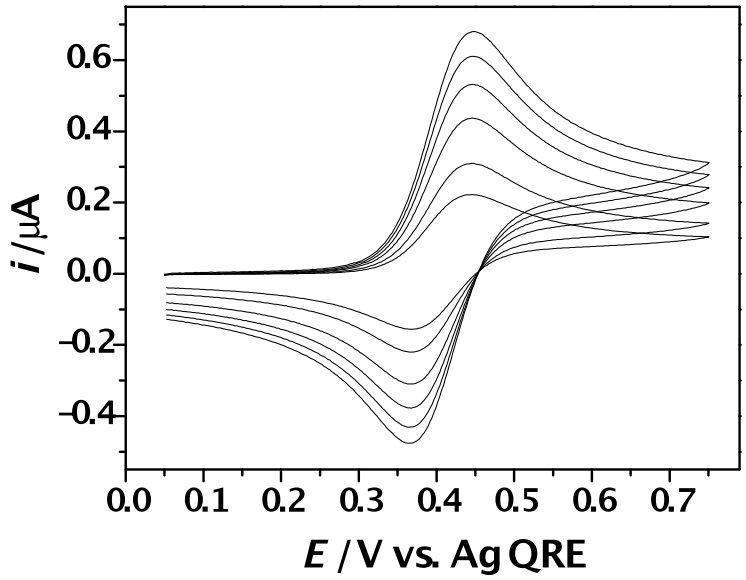

Figure S26 *CVs obtained at WE2 in a 4.56 mM solution of FcC_1Im in $[C_2C_1Im][Tf_2N]$, ν ranged from 25-500 mV s^{-1}, T = 298 K, p = 1 atm.*

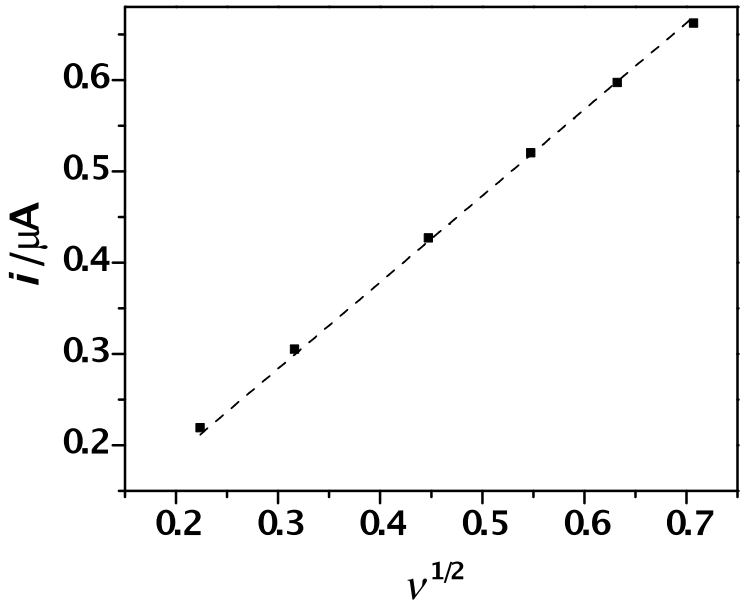

Figure S27 *Randles-Sevçik plots of $i_{p,a}$ vs. $\nu^{1/2}$ at T = 298 K.*

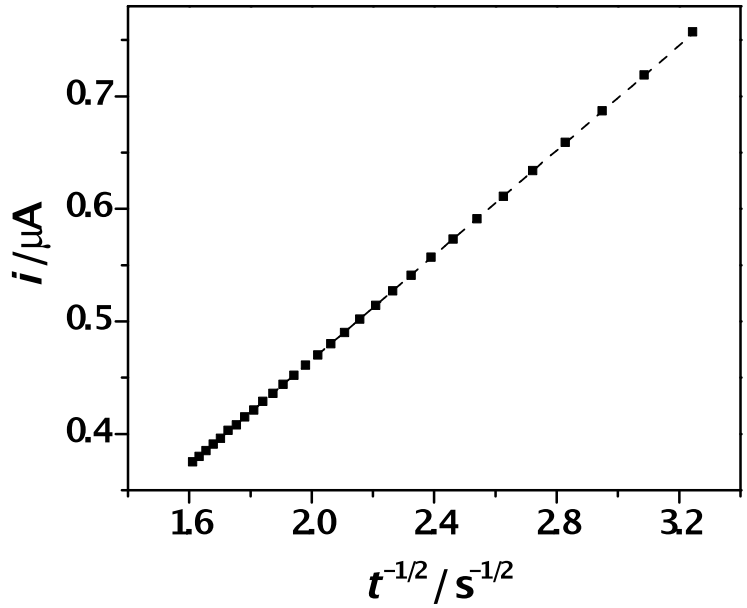

Figure S28 *Cottrell plot generated from the chronoamperometric curve recorded at WE2 in a 4.56 mM solution of FcC_1Im in $[C_2C_1Im][Tf_2N]$, T = 298 K, p = 1 atm.*

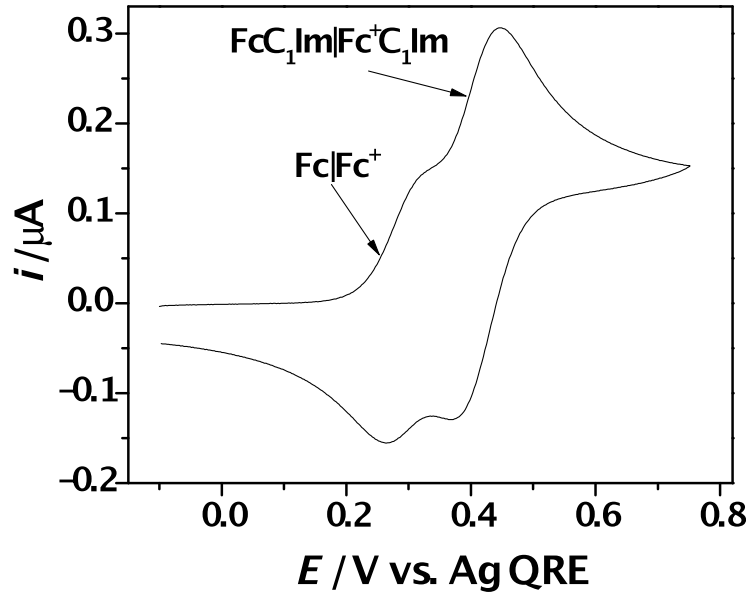

Figure S29 *CV recorded obtained at WE2 in a in a 4.56 mM solution of FcC_1Im in $[C_2C_1Im][Tf_2N]$ doped with 1.55 mM ferrocene, ν = 50 mV s^{-1}, T = 298 K, p = 1 atm.*

$[FcC_1NMe_3][Tf_2N]$ in $[C_2C_1Im][Tf_2N]$

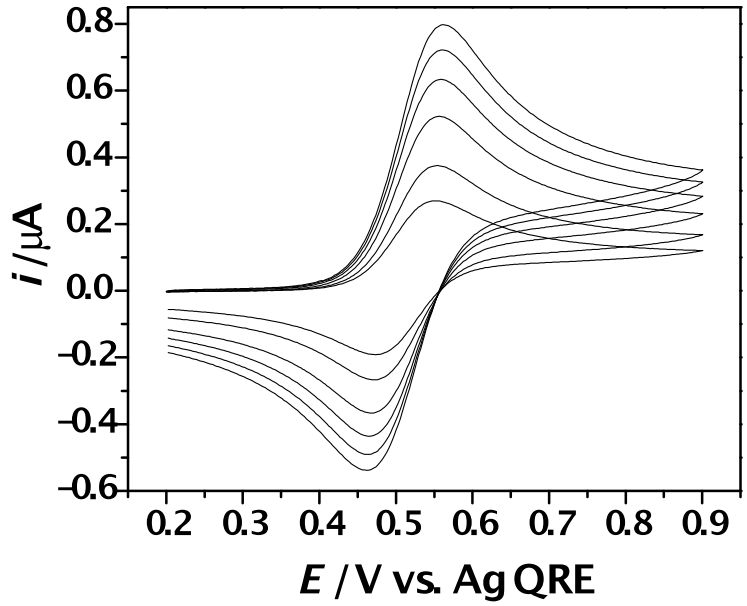

Figure S30 *CVs obtained at WE2 in a 4.79 mM solution of $[FcC_1NMe_3][Tf_2N]$ in $[C_2C_1Im][Tf_2N]$, ν ranged from 25-500 mV s^{-1}, T = 298 K, p = 1 atm.*

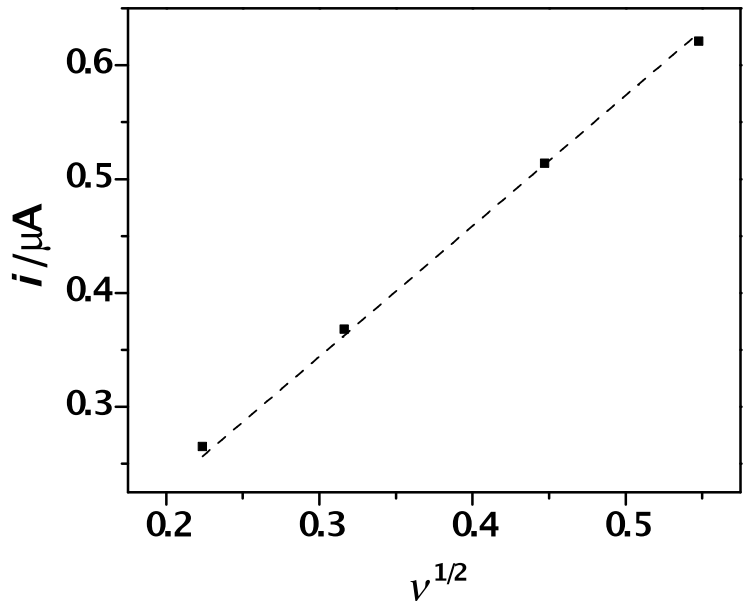

Figure S31 *Randles-Sevçik plots of $i_{p,a}$ vs. $\nu^{1/2}$ at T = 298 K.*

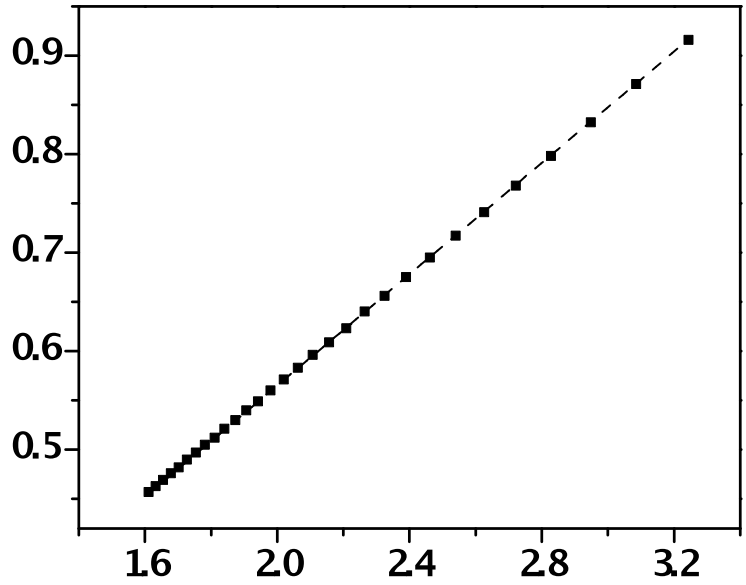

Figure S32 *Cottrell plot generated from the chronoamperometric curve recorded at WE2 in a 4.79 mM solution of $[FcC_1NMe_3][Tf_2N]$ in $[C_2C_1Im][Tf_2N]$, T = 298 K, p = 1 atm.*

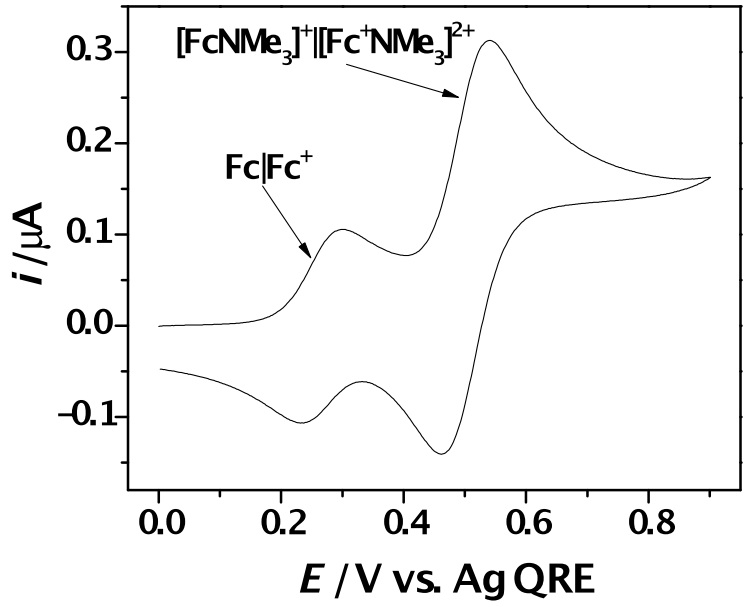

Figure S33 *CV recorded obtained at WE2 in a in a 4.79 mM solution of $[FcC_1NMe_3][Tf_2N]$ in $[C_2C_1Im][Tf_2N]$ doped with 1.25 mM ferrocene, ν = 50 mV s^{-1}, T = 298 K, p = 1 atm.*

Table S9 *Data used to calculate the hole radius, r_H, and correlation length, ζ, values presented in Figure 5.*

Ionic Liquid	T / K	γ / mN m^{-1}	r_H / Å	η / Pa s	D_{Cott} / $\times 10^{-7}$ cm^2 s^{-1}	ζ / Å
$[C_2C_1Im][Tf_2N]$	298	36.0	1.78	0.0342	1.71	3.73
	313	35.2	1.85	0.0203	2.70	4.18
	330	34.2	1.93	0.0131	4.05	4.55
	348	33.6	1.99	0.0083	5.91	5.19
	363	32.9	2.06	0.0058	7.99	5.73
$[C_4C_1Im][Tf_2N]$	298	32.6	1.87	0.0523	1.09	3.83
	313	31.9	1.94	0.0275	1.73	4.82
	330	30.8	2.03	0.0168	2.68	5.37
	348	30.4	2.10	0.0098	3.87	6.72
	363	29.1	2.19	0.0065	5.73	7.13
$[C_8C_1Im][Tf_2N]$	298	29.8	1.96	0.0955	0.68	3.34
	313	29.2	2.03	0.0459	1.50	3.33
	330	28.2	2.12	0.0258	1.89	4.95
	348	27.3	2.21	0.0134	3.44	5.53
	363	26.8	2.28	0.0085	4.55	6.87
$[C_4C_1Im][PF_6]$	298	45.9	1.58	0.2448	0.26	3.47
	313	44.7	1.64	0.1061	0.60	3.63
	330	43.4	1.71	0.0532	1.06	4.28
	348	42.0	1.79	0.0255	1.99	5.02
	363	40.8	1.85	0.0146	3.12	5.82
$[C_8C_1Im][PF_6]$	298	35.3	1.80	0.7032	0.09	3.56
	313	34.4	1.87	0.2632	0.20	4.33
	330	33.3	1.95	0.1008	0.45	5.30
	348	32.1	2.04	0.0395	0.88	7.31
	363	31.2	2.11	0.0194	1.47	9.29